Neurobiology of Disease

# RANBP17 Overexpression Restores Nucleocytoplasmic Transport and Ameliorates Neurodevelopment in Induced DYT1 Dystonia Motor Neurons

Masuma Akter,* Haochen Cui,* Md Abir Hosain,* Jinmei Liu, Yuntian Duan, and Baojin Ding
Department of Biochemistry and Molecular Biology, Louisiana State University Health Sciences Center at Shreveport, Shreveport, Louisiana 71130-3932

**DYT1 dystonia is a debilitating neurological movement disorder, and it represents the most frequent and severe form of hereditary primary dystonia. There is currently no cure for this disease due to its unclear pathogenesis. In our previous study utilizing patient-specific motor neurons (MNs), we identified distinct cellular deficits associated with the disease, including a deformed nucleus, disrupted neurodevelopment, and compromised nucleocytoplasmic transport (NCT) functions. However, the precise molecular mechanisms underlying these cellular impairments have remained elusive. In this study, we revealed the genome-wide changes in gene expression in DYT1 MNs through transcriptomic analysis. We found that those dysregulated genes are intricately involved in neurodevelopment and various biological processes. Interestingly, we identified that the expression level of RANBP17, a RAN-binding protein crucial for NCT regulation, exhibited a significant reduction in DYT1 MNs. By manipulating RANBP17 expression, we further demonstrated that RANBP17 plays an important role in facilitating the nuclear transport of both protein and transcript cargos in induced human neurons. Excitingly, the overexpression of RANBP17 emerged as a substantial mitigating factor, effectively restoring impaired NCT activity and rescuing neurodevelopmental deficits observed in DYT1 MNs. These findings shed light on the intricate molecular underpinnings of impaired NCT in DYT1 neurons and provide novel insights into the pathophysiology of DYT1 dystonia, potentially leading to the development of innovative treatment strategies.**

*Key words:* **dystonia; human-induced pluripotent stem cells (hiPSCs); motor neurons; neurodevelopment; nucleocytoplasmic transport; RANBP17; Torsin ATPase**

### Significance Statement

**DYT1 dystonia is a debilitating neurological movement disorder, and currently, there is no cure available due to its unclear pathogenesis. However, the inaccessibility of patient neurons greatly hinders the progress of research on this disease. In this study, we generated DYT1 patient–specific neurons from induced pluripotent stem cells and examined genome-wide changes in gene expression. We have identified that Ran-binding protein 17, a nuclear transport regulator, plays a substantial mitigating role, effectively rescuing cellular deficits observed in DYT1 neurons. These findings shed light on the intricate molecular underpinnings in DYT1 dystonia and have the potential to lead to the development of innovative treatment strategies.**

Received Sept. 11, 2023; revised Feb. 18, 2024; accepted Feb. 20, 2024.

Author contributions: B.D. designed research; M.A., H.C., M.H., J.L., Y.D., and B.D. performed research; M.A., H.C., and B.D. contributed unpublished reagents/analytic tools; M.A., H.C., and B.D. analyzed data; B.D. wrote the paper.

We thank the members of the Ding laboratory for their help and discussion. This work was supported by the NIH National Institute of Neurological Disorders and Stroke (NINDS; NS112910 and NS133252 to B.D.), Department of Defense (DoD) Peer Reviewed Medical Research Program (PRMRP) Discovery Award (W81XWH2010186 to B.D.), and LSU Health Shreveport Center for Brain Health (CBH) Grant in Aid (Spring 2022 to B.D.).

*M.A., H.C., and M.A.H. contributed equally to this work.

The authors declare no competing financial interests.

Correspondence should be addressed to baojin.ding@lsuhs.edu.

https://doi.org/10.1523/JNEUROSCI.1728-23.2024



## Introduction

Childhood-onset DYT1 dystonia is the most prevalent and severe form of hereditary primary dystonia characterized by involuntary muscle contractions, causing repetitive and often twisting movements or abnormal postures (Gonzalez-Alegre, 2019; Keller Sarmiento and Mencacci, 2021). This condition is notably recognized as a neurodevelopmental disorder due to its manifestation during childhood and adolescence, a pivotal phase for significant motor learning (Dauer, 2014; Pappas et al., 2018; Li et al., 2021). The majority of typical DYT1 dystonia cases arise from a heterozygous 3-bp deletion (ΔGAG) within exon 5 of

the *TOR1A* gene. This genetic alteration results in the elimination of a single glutamate residue from the C-terminal region of the Torsin 1A protein (ΔE; Ozelius et al., 1997; Charlesworth et al., 2013; Keller Sarmiento and Mencacci, 2021).

Torsin proteins belong to the evolutionarily conserved AAA+ (ATPase Associated with diverse cellular Activities) ATPase superfamily, which plays critical roles in a spectrum of essential biological processes (BPs), such as membrane trafficking, cytoskeleton dynamics, vesicle fusion, and response to stress (Ogura and Wilkinson, 2001; Hanson and Whiteheart, 2005; White and Lauring, 2007; Rampello et al., 2020). Most Torsin 1A proteins are embedded in the lumen of the endoplasmic reticulum (ER) and the nuclear envelope (NE; Vander Heyden et al., 2011). Experimental loss of torsin in various organisms, including mice (Goodchild et al., 2005), *Caenorhabditis elegans* (VanGompel et al., 2015), *Drosophila* (Jokhi et al., 2013), and mammalian cells (Naismith et al., 2004; Laudermilch et al., 2016; Ding et al., 2021), leads to abnormal NE morphology and developmental deficits. Despite evidence indicating that the ΔE mutation response to DYT1 dystonia is a loss-of-function alteration (Torres et al., 2004; Goodchild et al., 2005; Zhao et al., 2013), how it causes dystonia remains poorly understood.

Nucleocytoplasmic transport (NCT) is the process that tightly regulates the bidirectional communications between the nucleus and the cytoplasm across the NE (Hetzer, 2010; Ding and Sepehrimanesh, 2021; Park et al., 2022; Vorlander et al., 2022). Dysregulation of NCT has been shown to be implicated in development (Packard et al., 2015; Parra and Johnston, 2022), aging (Mertens et al., 2015), and many neurological diseases, including amyotrophic lateral sclerosis (Freibaum et al., 2015; Jovicic et al., 2015; Zhang et al., 2015; Kim and Taylor, 2017; Chou et al., 2018; Burk and Pasterkamp, 2019), Huntington's disease (Gasset-Rosa et al., 2017; Grima et al., 2017), Parkinson's disease (Chen et al., 2020), Alzheimer's disease (Eftekharzadeh et al., 2018; Lester and Parker, 2018), dystonia (Ding et al., 2021; Ding, 2022), and ataxia (Zhang et al., 2020). Generally, cargos with a mass of <45 kDa can passively diffuse through the nuclear pore complex (NPC). However, the transport of larger macromolecules through the NPC requires receptor-mediated transport pathways (Paci et al., 2020; Andreu et al., 2022). Each transport pathway typically involves distinct nuclear transport receptors, the small GTPase Ran (Ras-related nuclear protein), and its regulatory factors (Melchior et al., 1995; Moroianu and Blobel, 1995; Grunwald et al., 2011). Many nuclear transport receptors belong to the karyopherin families, which include importins, exportins, and biportins (Wing et al., 2022). Importins recognize nuclear localization sequences (NLS) on cargo proteins and facilitate their import into the nucleus. Exportins, on the other hand, identify nuclear export sequences (NES) and enable the export of cargo proteins (Lange et al., 2007; Stewart, 2007). These karyopherins bind to the NLS or NES of their cargos and the GTPase Ran. They subsequently mediate the association with phenylalanine and glycine repeats of nucleoporins (Nups) within the central channel of NPCs (Moore and Blobel, 1993; Fung and Chook, 2022).

Ran-binding proteins (RanBPs) are large scaffolding proteins that interact with Ran and Ran-GTPase–activating protein (RanGAP) to stimulate GTP hydrolysis (Seewald et al., 2002, 2003). In humans, there are >15 RanBPs, some of which overlap with Nups (e.g., RanBP2 also known as Nup358 (Delphin et al., 1997; Mahajan et al., 1997), importins (e.g., RanBP8 also known as importin 8 (Gorlich et al., 1997), or exportins (e.g., RanBP16 also known as exportin 7 (Kutay et al., 2000). Due to their anchoring on the cytoplasmic side of the nuclear membrane, RanBPs efficiently facilitate the conversion of RanGTP to RanGDP only within the cytoplasm. This leads to a nuclear-to-cytoplasmic ratio of RanGTP ∼200:1 (Barbato et al., 2020; Ding et al., 2020). The Ran cycle and the RanGTP–RanGDP gradient across the NE generate a propulsive force that drives directional NCT processes (Becskei and Mattaj, 2003; Kopito and Elbaum, 2007; Terry and Wente, 2009; Ding et al., 2020; Kalita et al., 2021). Thus, RanBPs are essential for maintaining the proper compartmentalization of cellular components (CCs) and ensuring efficient cellular processes.

Previously, we modeled DYT1 dystonia using patient-derived motor neurons (MNs). These patient-specific neurons retain the donor's heterozygous *TOR1A* mutation (ΔE) and show disease-dependent cellular deficits, including a deformed nucleus, disrupted neurodevelopment, and impaired NCT activities (Ding et al., 2021; Ding, 2022). These results suggested that torsin mutation (ΔE) may lead to widespread cellular dysregulation in DYT1 dystonia. To understand the genome-wide changes, we conducted a transcriptomic analysis to identify dysregulated genes using human MNs derived from DYT1-induced pluripotent stem cells (iPSCs). The dysregulated genes identified are extensively involved in neurodevelopment and various BPs. Intriguingly, we observed a significant decrease in the expression level of Ran-binding protein 17 (RANBP17) in DYT1 MNs compared with healthy controls. Through the manipulation of RANBP17 expression using shRNAs, we further demonstrated that RANBP17 plays a crucial role in the nuclear transport of both protein and transcript cargos in induced human neurons. Overexpression of RANBP17 substantially ameliorated the impaired NCT activity and rescued the neurodevelopmental deficits of DYT1 MNs. These findings elucidate the molecular mechanisms underlying the impaired NCT activities in DYT1 cells and provide novel insights into the pathophysiology of DYT1 dystonia.

## Materials and Methods

*Cell lines and culture condition.* HEK 293T cells (CRL-11268) were purchased from ATCC and cultured in DMEM supplemented with 10% fetal bovine serum (FBS, Corning) and 1% penicillin/streptomycin. Human-induced pluripotent stem cell (hiPSC) lines have been generated in our previous studies, including a DYT1 patient–derived hiPSC and age-matched healthy control hiPSC line (Ding et al., 2021), a set of hiPSC lines carrying a heterozygous or homozygous GAG deletion in the *TOR1A* gene and their isogenic wild-type controls (Akter et al., 2021), and a set of gene-corrected isogenic control lines that were generated from a DYT1 patient hiPSC line (Akter et al., 2022a). All hiPSCs were maintained in complete mTeSR1 medium (STEMCELL Technologies) on Matrigel (Corning)-coated dishes at 37°C and 5% $CO_2$ with saturating humidity, and the medium was replaced daily.

The recipes of other culture media used in this study are:

1. Neuronal maturation medium: DMEM:F12:neurobasal (2:2:1), 0.8% N2 (Invitrogen), 0.8% B27 (Invitrogen), and 1% penicillin/streptomycin, supplemented with 5 mM FSK and 10 ng/ml each of BDNF, GDNF, and NT3 (PeproTech).
2. KOSR medium: DMEM/F12 medium with 20% KnockOut Serum Replacement (KOSR; Thermo Fisher Scientific), 1% GlutaMax, 1% nonessential amino acid (NEAA), 50 μM β-mercaptoethanol (β-ME), 1% P/S, and 10 ng/ml basic fibroblast growth factor (bFGF; PeproTech).
3. Neurosphere medium (NSP medium): DMEM/F12 medium containing 1% N2, 1% GlutaMax, 1% NEAA, 50 μM β-ME, 1% P/S, 8 μg/ml heparin, 20 ng/ml bFGF, and 20 ng/ml epidermal growth factor (EGF; PeproTech).

4. Neural progenitor cell medium: DMEM/F12 and neurobasal medium (1:1) containing 0.5% N2 (Invitrogen), 1% B27 (Invitrogen), 1% GlutaMax, 1% NEAA, 50 μM β-ME, 1% P/S, 10 ng/ml EGF, and 10 ng/ml bFGF.

*Plasmid construction and lentivirus production.* A third-generation lentiviral vector (*pCSC-SP-PW-IRES-GFP*) was used to express GFP and RFP reporters. PCR-amplified GFP-NES, GFP-NLS, RFP-NES, and RFP-NLS sequences were ligated into the lentiviral vector between the BamHI (5′) and XhoI (3′) restriction sites. The cDNA of RANBP17 was purchased from GenScript. The same lentiviral vector was used to express GFP-tagged RANBP17. The PCR-amplified GFP sequence and the full-length RANBP17 sequence were ligated into the lentiviral vector via Gibson assembly (New England Biolabs). Another third-generation lentiviral vector (*LV-CAG-mCherry-miRE-Luc*) was used to express *TOR1A-shRNAs* and *RANBP17-shRNAs* as described in the previous report (Pelossof et al., 2017; Ding et al., 2021). Briefly, shRNA oligos targeting the gene coding regions were synthesized (Integrated DNA Technologies), PCR-amplified with flanking miR-30 sequences, and ligated into the above lentiviral vector at the *XhoI* and *EcoRI* restriction sites. The targeting sequences are AACGGTGTT CACCAAGTTAGAT (*TOR1A*-shRNA-1), CAGCAAGATCATCGCA GAGAATA (*TOR1A*-shRNA-2), GTAGGAGGAAGATTAACATATA (*RANBP17*-shRNA-1), and AAACAGTATTACAAATATTCAA (*RA NBP17*-shRNA-2). All plasmids were verified by restriction enzyme digestions and DNA sequencing.

Each of these vectors was cotransfected with packaging plasmids (Addgene #12251, #12253, and #12259) into HEK293T cells for virus production (Dull et al., 1998; Zufferey et al., 1998). Replication-incompetent lentiviruses were produced, and viral supernatants were collected at 48 and 72 h post-transfection as previously described (Ding and Kilpatrick, 2013; Sepehrimanesh et al., 2021). The viral supernatants were filtered using 0.45 μm syringe filters and stored at 4°C prior to cell transduction.

*Generation of hiPSC-derived MNs.* MNs were prepared from hiPSCs as previously described (Sepehrimanesh and Ding, 2020; Ding, 2021; Akter et al., 2022b). Briefly, hiPSCs were cultured in mTeSR1 medium with 10 μM all-trans retinoic acid (Sigma-Aldrich) and 0.5 mM VPA in Matrigel-coated six-well plates for 7 d. Cells were then digested with Versene and gently resuspended as small aggregates in KOSR medium with 10 μM Y-27632 (STEMCELL Technologies). Cell clumps were cultured in KOSR medium for 4 d, followed by the culture in NSP medium for another week. The NSPs were then dissociated into single cells with Accutase (Innovative Cell Technologies) and maintained in a neural progenitor cell medium. For MN differentiation, neural progenitor cells were plated into Matrigel-coated plates at a density of $3 \times 10^4$ cells/cm$^2$ and transduced with a lentivirus expressing *NEUROG2-IRES-ISL1-T2A-LHX3* (Sepehrimanesh and Ding, 2020; Akter et al., 2022b; Akter and Ding, 2022). The culture medium was replaced the next day with a neuronal maturation medium. Neurons were dissociated with Accutase on Day 5 and replated onto Matrigel-coated coverslips with or without the presence of astrocytes depending on the desired experiments. The medium was half changed twice a week until analysis.

*Quantitative real-time PCR analysis.* Total RNA was extracted from cultured cells using TRIzol (Life Technologies), and genomic contamination was removed using TURBO DNase (Life Technologies). cDNA synthesis reactions were performed using 0.5 μg of RNA from each sample with the SuperScript III First-Strand kit (Life Technologies) and random hexamer primers. Real-time PCR was performed in triplicate using primers, SYBR Green ER SuperMix (Invitrogen), and the Bio-Rad CFX-96 Fast Real-Time PCR system. Target mRNA levels were normalized to the reference gene *GAPDH* by the $2^{-\Delta\Delta Ct}$ method as described previously (Ding et al., 2013, 2016, 2018). The sequences of RT-PCR primers (from 5′ to 3′) are GCAGAACCTGTCCGTCAAGA (RANBP17-F), CTGCATGGTTCAGTGTTGCC (RANBP17-R), CAAA TTCCATGGCACCGTCA (GAPDH-F), and GGACTCCACGACGTA CTCAG (GAPDH-R), AATACTGGCTCTGCGATGCT (SYN1-F), TGA CCACGAGCTCTACGATG (SYN1-R), AAACATGCTGATCCCCTCAG (VGLUT1-F), AACCACAAAAGGCTGTCGTC (VGLUT1-R), AGGG ACTTGTTGAGGGTGTG (VGLUT2-F), CTGCACAAGAATGCCAG CTA (VGLUT2-R), CTTACGGAGCGGTCGTGTAT (NEUN-F), TCACATGGTTCCAATGCTGT (NEUN-R), CACCCAGCAGATG TTCGAT (TUBB3-F), and CTGTTCTTGCTCTGGATGGC (TUBB3-R).

*RNA sequencing and bioinformatic analyses.* The total RNA was extracted from cultured cells and purified using PureLink RNA Mini Kit (Invitrogen) according to the manufacturer's instructions. The RNA integrity was determined by the Agilent 2100 BioAnalyzer (Agilent Technologies) and sequenced using the Illumina NovaSeq (Novogene).

The data obtained in FASTQ file format from RNA sequencing were aligned to Ensembl hg38 human genome using the HISAT2 program. Gene-level abundances were estimated as FPKMs (Fragments Per Kilobase of transcript sequence per Million base pairs sequenced). The read count summarization to each gene (i.e., counts) was calculated using featureCounts. Analyses of differential expression of transcripts were performed with DESeq2(1.20.0). Genes with a false discovery rate (FDR) value of <1% and log2 fold change (FC) ≥1 were considered to be differentially expressed genes (DEGs). The resulting *p*-values of differential expression were accompanied by respective FC values. The *p*-values were adjusted for multiple testing by calculating the FDR by Benjamini and Hochberg's method. Volcano plots and heat maps were created using the Rgplot and ggplot2 in Rstudio v1.1.463 (Anders and Huber, 2010; Walter et al., 2015). FCs >1.5 and *p*-value <0.05 were considered the cutoff values for identifying upregulated and downregulated DEGs.

*Immunocytochemistry (ICC).* Cultured cells at the indicated time points were fixed with 4% paraformaldehyde (PFA) in PBS for 15 min at room temperature (RT) and then permeabilized and blocked for 1 h in a blocking buffer (PBS containing 0.2% Triton X-100 and 3% BSA). They were subsequently incubated overnight with primary antibodies in a blocking buffer at 4°C, followed by washing and incubation with corresponding fluorophore-conjugated secondary antibodies. Cell nuclei were counterstained with Hoechst (HST) 33342 (Thermo Fisher Scientific). The primary antibodies used in this study were TUBB3 (Covance, MMS-435P, or PRB-435P-100, 1:2,000).

*Neurodevelopmental assay.* For neurite outgrowth assay, iPSC-derived neurons were fixed at the desired time points and stained with TUBB3. The neurite length was measured by the ImageJ software (NIH) based on TUBB3 signals as described previously (Ding et al., 2013, 2016, 2018). For branch assay, based on confocal images with TUBB3 staining, neurites with direct connection with the soma were counted as primary branches, and neurites directly connected with primary branches were considered as secondary branches. The numbers of primary and secondary branches were counted as previously described (Ding et al., 2021).

*Fluorescence in situ hybridization (FISH).* FISH was performed as described previously (Ding et al., 2020; Cui et al., 2022). Briefly, cultured cells were washed once with PBS and fixed with 4% PFA for 30 min at RT. Cells were permeabilized with 0.2% Triton X-100 for 10 min, followed by two washes with PBS. Samples were equilibrated with a hybridization buffer composed of 2× SSC, 10% dextran sulfate, 10 mM ribonucleoside vanadyl complex (New England Biolabs), and 20% formamide. A mixture of digoxigenin (DIG)-labeled oligo-dT or dA probes (0.2 ng/μl) and yeast tRNA (0.2 μg/μl) was heated at 95°C for 5 min and immediately chilled on ice. Probes were then combined with equal volumes of 2× hybridization buffer and incubated with samples overnight at 37°C. Anti-DIG antibody (Sigma-Aldrich, 11333089001, 1:100) and corresponding fluorophore-conjugated secondary antibodies (Thermo Fisher Scientific) were used to detect oligo-dT signals. HST 33342 was used to stain the nuclei. All reagents and solutions were prepared in nuclease-free water.

*Protein nuclear transport assay.* Protein nuclear transport was analyzed using individual reporters expressing GFP-NES, GFP-NLS,

RFP-NES, or RFP-NLS (Mertens et al., 2015; Cui et al., 2022). Neural progenitor cells derived from hiPSC were cotransfected with lentiviruses expressing MN reprogramming factors, transport reporters, GFP- or GFP-tagged RANBP17, or RANBP17-shRNAs in the desired experiments. The signal densities and distributions of GFP or RFP were analyzed as previously described (Ding et al., 2020; Cui et al., 2022).

*Confocal microscopy and image analysis.* Confocal images were obtained with a Nikon A1R or Zeiss LSM700 (63×/1.4 NA) confocal microscope. For fluorescence intensity quantification in FISH and reporter assay, we zoomed in on individual neurons using the ImageJ software, and as large an area as possible was measured within the nucleus or cytoplasm as previously described (Ding et al., 2020; Cui et al., 2022). An unbiased approach for data collection was employed. The person who analyzed the images was completely blinded to the sample information. The "mean" values were used to quantify an average signal density. For FISH assays, the average of oligo-dT signals in both the nucleus and cytoplasm were measured, and the ratio of nuclear to cytoplasmic oligo-dT signals ($dT_{nuc}/dT_{cyt}$) was used to evaluate the mRNA export. For the reporter assay, GFP or RFP signals were measured in the nucleus and cytoplasm. The ratio of nuclear to cytoplasmic GFP-NES or RFP-NES was used to evaluate protein export, while the ratio of cytoplasmic to nuclear GFP-NLS or RFP-NLS was used to measure the protein nuclear import.

*Western blotting analysis.* Cells were lysed in a lysis buffer composed of 50 mM Tris-HCl buffer (pH 8.0), 150 mM NaCl, 1% NP40, 1% Triton X-100, 0.1% SDS, 0.5% sodium deoxycholate, and protease inhibitor cocktail (Roche). Equal amounts of cell lysates (20 µg per lane) were used for SDS-PAGE and Western blot analysis as previously described (Ding et al., 2010, 2013). The primary antibodies and dilutions were actin (Sigma-Aldrich, A5441, 1:2,000), GFP (Santa Cruz Biotechnology, sc-9996, 1:250), and RANBP17 (Bethyl Laboratories, A303-994A, 1:500). HRP-conjugated secondary antibodies and Clarity Western ECL substrate (Bio-Rad) were used to visualize the protein bands with a Bio-Rad ChemiDoc.

*Statistical analysis.* Statistical analysis was done in GraphPad Prism. Unpaired two-tailed Student's *t* tests were used to compare one experimental sample with its control. One-way ANOVA was used when comparing multiple samples, with either Tukey's (when comparing samples with each other) or Dunnett's (when comparing samples to a control) post hoc tests. The results are expressed as mean ± SEM of at least three biological replicates, and $p < 0.05$ is considered as significant.

## Results

### Identification of dysregulated genes in human DYT1 MNs

We previously modeled DYT1 dystonia using patient-derived MNs (Ding et al., 2021). These human neurons retain the heterozygous *TOR1A* mutation and recapitulate disease-dependent cellular deficits, including impaired neurodevelopment, a deformed nucleus, and disrupted NCT, resulting in the nuclear accumulation of mRNAs and mislocalized proteins (Ding et al., 2021; Ding, 2022). This study underscores the significance of patient-derived neurons in modeling neurological disorders and suggests that the torsin mutation (ΔE) might trigger widespread cellular dysfunction in DYT1 dystonia. To understand the genome-wide changes in gene expression, we conducted a transcriptomic study to identify dysregulated genes in DYT1 MNs. These MNs can be generated using our established protocols based on the induction and differentiation of hiPSCs (Sepehrimanesh and Ding, 2020; Akter et al., 2022b; Akter and Ding, 2022). The DYT1 iPSCs and healthy controls were induced to neuron progenitor cells and subsequently transduced with lentiviruses expressing three transcription factors essential for inducing neuron progenitor cells to MNs (Sepehrimanesh and Ding, 2020; Akter et al., 2022b). The high yield and purity of these iPSC-MNs enabled us to prepare total RNAs and perform transcriptomic studies (Fig. 1*A*,*B*).

Bioinformatic analysis identified 1,288 DEGs among 10,256 hits, consisting of 589 downregulated genes and 699 upregulated genes in DYT1 MNs when compared with healthy controls (Fig. 1*C*,*D*). These DEGs encompass a range of intriguing targets. For example, the *LMNB1* gene, which encodes the major nuclear lamina protein lamin B1, exhibits significant upregulation (Fig. 1*E*), consistent with our previous discovery that nuclear lamin B1 experiences dysregulation both in terms of expression and subcellular localization in DYT1 MNs (Ding et al., 2021). The *EIF2A* gene, which encodes the eukaryotic translation initiation factor 2A, is downregulated more than twofold in DYT1 neurons (Fig. 1*E*), agreeing with the previous study that the impaired eIF2alpha signaling is a generalized mechanism for dystonia (Rittiner et al., 2016). These consistent results validate the reliability of the transcriptomic study using reprogrammed DYT1 neurons. Additionally, we observed a significant increase in Torsin 1A–interacting protein 1 (TOR1AIP1), an essential cofactor for Torsin 1A function (Laudermilch and Schlieker, 2016), in DYT1 neurons (Fig. 1*E*). This upregulated TOR1AIP1 expression in DYT1 neurons could potentially result from a feedback to the impairment of the interaction between the Torsin mutant and its binding partners (Naismith et al., 2009).

### Dysregulated genes in human DYT1 MNs are comprehensively involved in neurodevelopment and various BPs

The results of Gene Ontology (GO) analysis indicate that these DEGs are primarily associated with BPs including regulation of gene expression, neuron differentiation and development, and protein and RNA transport and localization (Fig. 2*A*). The products of these DEGs are widely distributed across various CCs, with notable enrichment in membrane-bound organelles such as synapse, ER membrane and lumen, Golgi apparatus and membranes, mitochondrial and inner membranes, postsynaptic membranes, and the NE (Fig. 2*A*). The related molecular functions (MFs) encompass ATP binding (Fig. 2*E*), protein binding, transcription factors (Fig. 2*D*), calcium ion binding, GTPase activity, and calmodulin binding, among others. The involved KEGG pathways include the ECM–receptor interaction pathway (Fig. 2*G*), TGF-β signaling pathway, MAPK signaling pathway, calcium signaling pathway, neurotrophin signaling pathway, axon guidance, and glutamatergic synapse (Fig. 2*F*). Thus, when compared with healthy controls, DYT1 neurons exhibit comprehensive functional alterations in signaling transduction, gene expression, and transport regulation (Fig. 2*A*).

We also conducted a GO analysis of both downregulated and upregulated genes. The downregulated genes show substantial enrichment in BPs closely associated with neurodevelopment and functions. These processes include central nervous system development, positive regulation of transcription, nerve growth factor receptor signaling pathway, EGF receptor signaling pathway, migration, and axon guidance, among others (Fig. 2*B*). On the other hand, the upregulated genes are significantly enriched in BPs involving cellular protein metabolic process and posttranslational protein modification (Fig. 2*C*). These DEGs align with the known functions of Torsin ATPase, which participates in diverse cellular activities such as membrane trafficking, cytoskeleton dynamics, vesicle fusion, protein control, and nuclear transport. This suggests the presence of intricate pathophysiological mechanisms underlying DYT1 dystonia.

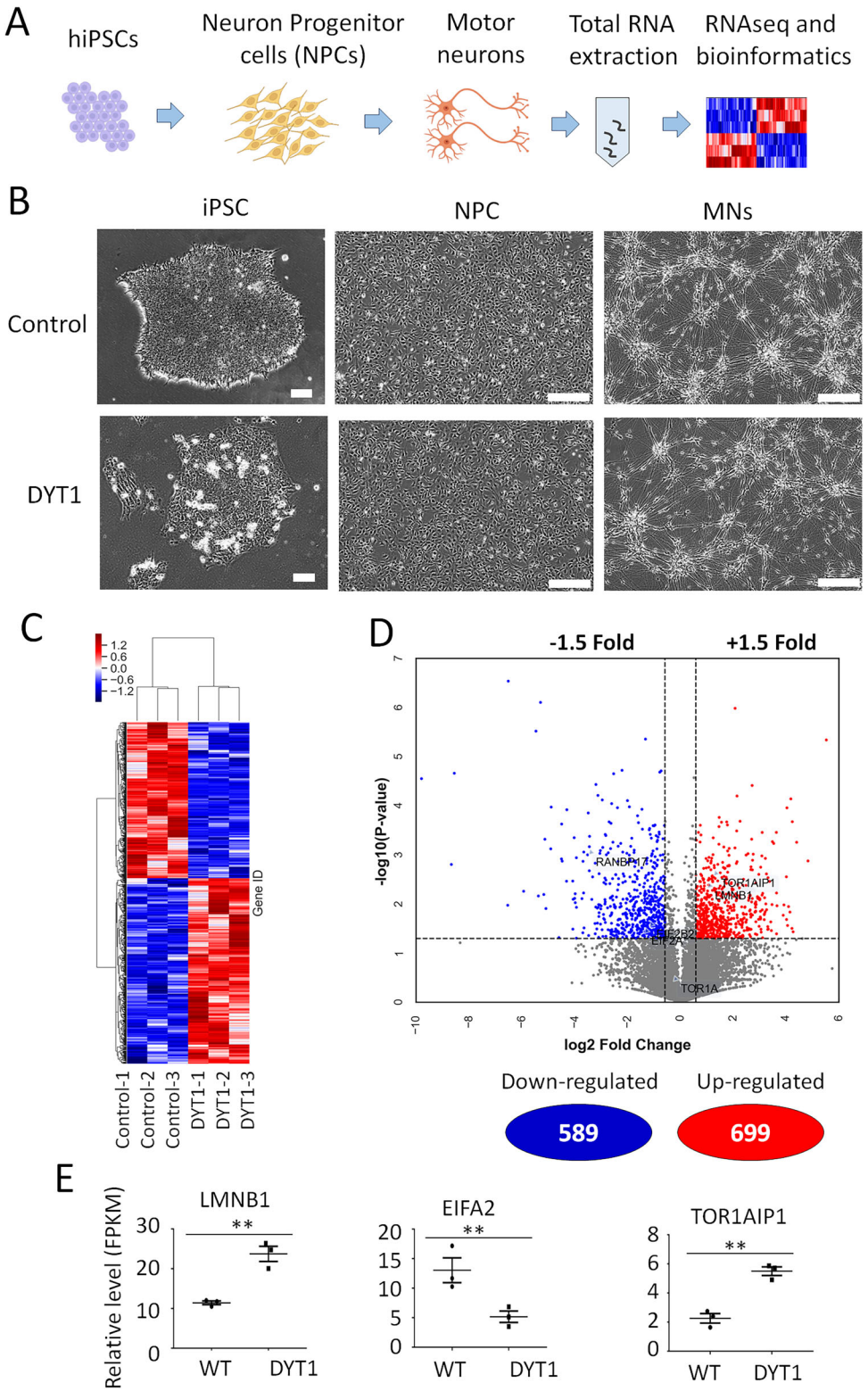


**Figure 1.** Identification of dysregulated genes in human DYT1 MNs. ***A***, Schematic shows the workflow of identification of dysregulated genes from iPSC-derived MNs. ***B***, Representative micrographs of cells at different stages during the generation of human MNs. iPSCs, induced pluripotent stem cells; NPCs, neuronal progenitor cells; and MNs, motor neurons. Scale bar, 100 µm. ***C***, Heat map of RNAseq results of DEGs in DYT1 MNs compared with healthy controls. ***D***, Volcano plot shows the upregulated and downregulated DEGs in DYT1 MNs. Six hundred ninety-nine genes (in red) were upregulated, and 589 genes (in blue) were downregulated. ***E***, Some interesting targets have been identified with disrupted gene expression in DYT1 MNs. FPKM, Fragment Per Kilobase of Million mapped read. $^{**}p < 0.01$. Student's *t* tests.

We observed that certain DEGs in DYT1 MNs cluster into groups with specific functions. Homeobox genes, a class of transcription factors critical for developmental processes such as regional specification, patterning, and differentiation (Duverger and Morasso, 2008; Lim, 2023), are significantly downregulated in DYT1 MNs (Fig. 2*D*). For example, the *TLX1* gene, which

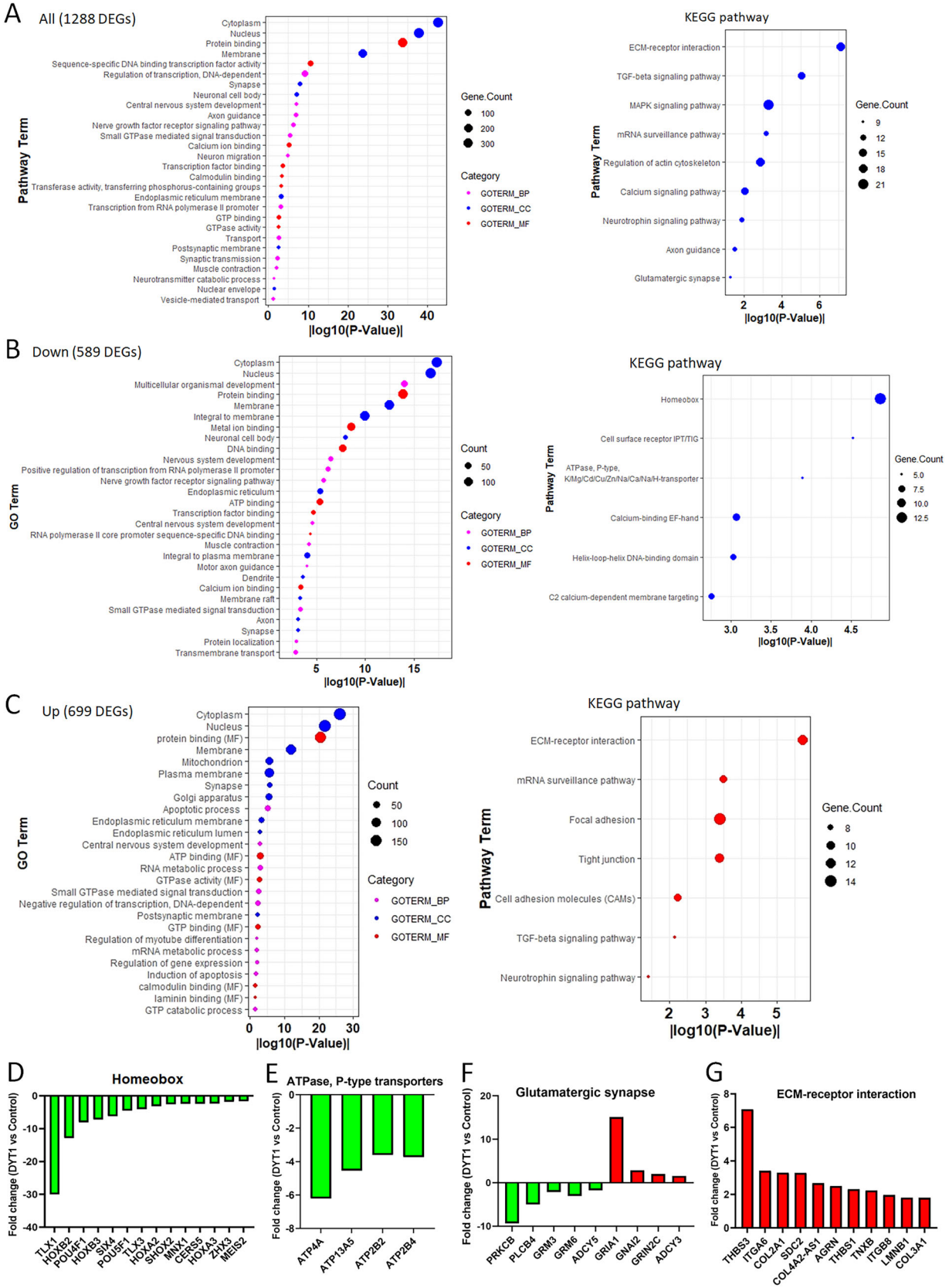


**Figure 2.** Dysregulated genes in human DYT1 MNs are comprehensively involved in neurodevelopment and various BPs. ***A***, GO analysis of all significant DEGs in DYT1 MNs. Some terms of BP, CC, and MF and KEGG pathways were presented. ***B***, Representative results of GO analysis and KEGG pathways of significantly upregulated genes in DYT1 MNs. ***C***, Representative results of GO analysis and KEGG pathways of significantly downregulated genes in DYT1 MNs. ***D–G***, Some groups of DEGs, including downregulated homeobox genes (***D***), downregulated ATPases (***E***), down- and upregulated glutamatergic synapse-related genes (***F***), and mostly upregulated enriched genes in the KEGG pathway of the ECM–receptor interaction (***G***).

encodes a nuclear transcription factor involved in spinal cord development and the specification of neuronal cell fates (Cheng et al., 2004; Xu et al., 2008; Guo et al., 2012), exhibits approximately 30-fold decrease in DYT1 MNs compared with healthy controls (Fig. 2*D*). Interestingly, a recent report using DYT1 mouse model found that conditional knock-out *Tor1a* in spinal cord MNs, not dorsal root ganglia (DRGs), resulted in early-onset dystonia (Pocratsky et al., 2023). The findings from this study, coupled with our transcriptomic results, suggest that dysregulation of neurodevelopment, including spinal cord MNs, may constitute a major pathogenic factor in DYT1 dystonia.

The dysregulation of other gene groups, such as ATPase transporters (downregulated; Fig. 2*E*) and the glutamatergic synapse (with some genes downregulated and others upregulated; Fig. 2*F*), may significantly impact the maturation and function of DYT1 MNs. Notably, upregulated genes are highly enriched in the KEGG pathway of the ECM–receptor interaction (Fig. 2*C*,*F*). ECM–receptors and their ligands play a key role in neurodevelopment as guidance molecules, influencing neurons for axonal growth, dendritic projections, and synaptogenesis (Kerrisk et al., 2014). Dysregulation of these genes may disrupt cell-to-cell and cell-to-matrix interactions, leading to dysfunction in synaptic activity and behavior. However, the implication of the ECM–receptor interaction in the pathogenesis of DYT1 dystonia has received little attention. Overall, our transcriptomic study provides a comprehensive understanding of the genome-wide changes in gene expression in DYT1 neurons. The dysregulated genes and pathways offer novel insights into the disease's pathogenesis and present crucial targets for further investigation in deciphering the detailed pathophysiology of the condition.

### RANBP17 expression decreased in DYT1 MNs

RANBP17 is considered a member of the importin-β superfamily of nuclear transport receptors (Kutay et al., 2000; Mertens et al., 2015). Although RANBP17 is expected to play an important role in NCT activities, its detailed function in the regulation of different nuclear transport pathways remains undefined. In the result of transcriptomic study, the expression of RANBP17 was decreased >10-fold in DYT1 neurons compared with controls (Fig. 3*A*). Interestingly, RANBP17 showed specific dysregulation in DYT1 MNs, as other RANBP genes showed either a very mild change (e.g., RANBP1 and RANBP2) or no significant difference (e.g., RANBP3, RANBP6, and RANBP10; Fig. 3*A*). We further verified this change via two approaches. First, we conducted Western blotting and confirmed that RANBP17 protein levels dramatically decreased in DYT1 MNs compared with healthy controls (Fig. 3*B*). Second, we prepared MNs from more DYT1 iPSC lines, including the heterozygous and homozygous GAG deletion from a healthy iPSC line (Akter et al., 2021) and the genomically corrected GAG deletion from a patient iPSC line (Akter et al., 2022a). Using these iPSC-MNs, RANBP17 expression levels were measured via RT-PCR assay. We found that RANBP17 mRNA levels were significantly decreased in MNs carrying DYT1 GAG deletions, and the expression levels can be largely restored in GAG deletion-corrected isogenic controls (Fig. 3*C*). Moreover, in healthy MNs with downregulated *TOR1A* using shRNAs (Ding et al., 2021), RANBP17 expression significantly decreased (Fig. 3*C*). These results further confirmed that the decreased *RANBP17* expression is caused by the disruption of the *TOR1A* gene. To further examine the roles of RanBP17 in the regulation of NCT, we constructed four lentiviral vectors expressing GFP or RFP reporters that are fused with NES or NLS (Fig. 3*D*). Their expression and subcellular distribution have been validated in HEK cells (Fig. 3*D*). These individual reporters will be used to measure the NCT activities under different conditions in the following studies.

### Downregulation of RANBP17 interferes with protein NCT in induced human MNs

Considering the evident impairment of NCT in DYT1 neurons (Ding et al., 2021) and the expected roles of RANBP17 in NCT regulation, we hypothesized that decreased levels of RANBP17 might contribute to the impaired NCT activities in DYT1 neurons. To further examine the involvement of RANBP17 in NCT, we constructed lentiviral vectors expressing shRNAs to downregulate RANBP17 expression. The cells expressing shRNAs were identified by the mCherry reporter, with scrambled sequence shRNAs serving as a control. Two distinct shRNAs against RANBP17 were employed, both of which effectively downregulated the protein levels (Fig. 4*A*). As lentiviral vectors expressing RANBP17-shRNAs contain mCherry reporter, GFP-NES and GFP-NLS were used to measure the protein nuclear export and import, respectively (Fig. 4*B*). In healthy neuronal progenitor cells cotransduced with reprogramming factors, shRNAs, and transport reporters, subsequent induction led to the differentiation into MNs. Control MNs expressing the vector showed predominantly nuclear localization of the GFP-NLS reporter. In sharp contrast, MNs expressing RANBP17-shRNAs exhibited substantial GFP signals in the cytoplasm (Fig. 4*C*), resulting in a significant increase in the cytoplasmic-to-nuclear GFP signal ratio (Fig. 4*D*). This suggests impaired protein nuclear import in MNs with reduced RANBP17 levels. Similarly, we assessed protein nuclear export using GFP-NES. The control MNs exhibited exclusive cytoplasmic localization of GFP-NES, while MNs expressing RANBP17-shRNAs displayed substantial GFP signals in the nucleus (Fig. 4*E*,*F*). Overall, the downregulation of RANBP17 significantly disrupts both protein nuclear import and export.

### Downregulation of RANBP17 interferes with mRNA export

To investigate the impact of downregulation of RANBP17 on nuclear mRNA export, we performed FISH using oligo-dT probes, as previously reported (Ding et al., 2020, 2021; Cui et al., 2022). Healthy hiPSC-derived MNs expressing the respective shRNAs were identified by their coexpressed mCherry reporter. While the majority of mRNAs were found in the cytoplasm of iMNs infected with the vector control, iMNs expressing RANBP17 exhibited a substantial amount of oligo-dT signal inside the nucleus (Fig. 5*A*). The ratio of nuclear to cytoplasmic oligo-dT signal was significantly higher in iMNs expressing RANBP17-shRNAs (Fig. 5*B*), suggesting that the downregulation of RANBP17 also interferes with nuclear mRNA export.

### Downregulation of RANBP17 disrupts neurite outgrowth and neuron maturation

The impaired nuclear mRNA export in neurons with reduced RANBP17 levels could potentially impede protein synthesis and lead to delayed neurodevelopment and maturation (Ding, 2015). To test this, we employed healthy iMNs with lentiviruses expressing RANBP17-shRNAs (Fig. 4*A*). The infected neurons can be identified with the mCherry reporter (Fig. 6*A*). We measured the neurite outgrowth of iMNs at the early developmental stage of 7 d postviral infection (dpi) as previously reported (Ding et al., 2013, 2016, 2018). Compared with MNs expressing control

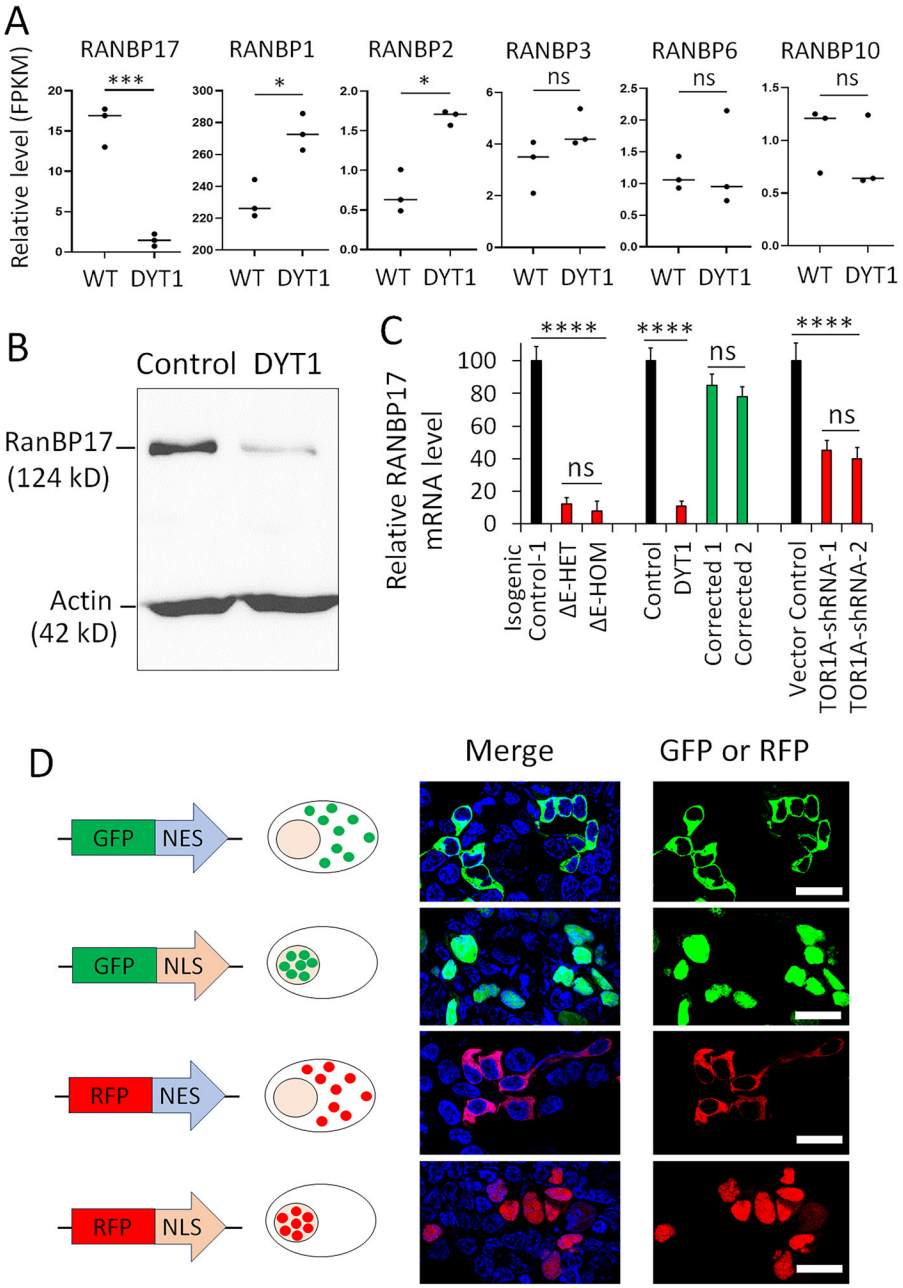


**Figure 3.** RANBP17 expression decreased in DYT1 neurons. ***A***, The expression levels of different RANBP genes in WT and DYT1 MNs from transcriptomic study. ns, no significant difference; *$p < 0.05$; ***$p < 0.001$. Student's *t* tests. ***B***, Western blotting shows the indicated protein levels of whole-cell extracts from healthy and DYT1 iPSC-MNs. RANBP17 and β-actin were sequentially probed on the same blot. ***C***, RT-PCR analysis of RANBP17 gene expression levels in MNs generated from indicated two groups of hiPSC lines and healthy MNs with downregulated RANBP17. ns, not significant; ****$p < 0.0001$. *N*, three replicates. Student's *t* tests. ***D***, Constructions of lentiviral vectors expressing transport reporters and the validation of their subcellular distribution in HEK cells. HST 33342 was used to stain nuclei. Scale bar, 25 µm.

vectors, MNs expressing RANBP17-shRNAs exhibited considerably shorter neurite length (Fig. 6*A*,*B*).

To further examine the impacts of RANBP17 on neuron maturation, we prepared RNA samples from iMNs at late stages of 14 and 21 dpi. At the time of sample collection, most iMNs were mCherry positive and showed healthy growth (Fig. 6*C*). Some genes related to neuron maturation have been analyzed by RT-PCR. These genes include SYN1, which encodes synapsin proteins implicated in synaptogenesis and the modulation of neurotransmitter release (Sansevrino et al., 2023), the genes encoding vesicular glutamate transporters (VGLUT1 and VGLUT2; El Mestikawy et al., 2011), and the RNA-binding fox-1 homolog 3, also known as NeuN antigen, which has been widely used as a marker for postmitotic neurons (Duan et al., 2016). After normalization with the neuron-specific marker TUBB3, we found that the expression levels of SYN1, VGLUT1, and VGLUT2 significantly decreased in iMNs with downregulated RANBP17 compared with controls (Fig. 6*D*). No significant differences were observed for NeuN. Thus, our results so far indicate a crucial role for RANBP17 in facilitating the nuclear transport of both protein and mRNA cargos. The downregulation of RANBP17 has a substantial impact on NCT activities and poses an interference in neurite outgrowth and neuron maturation.

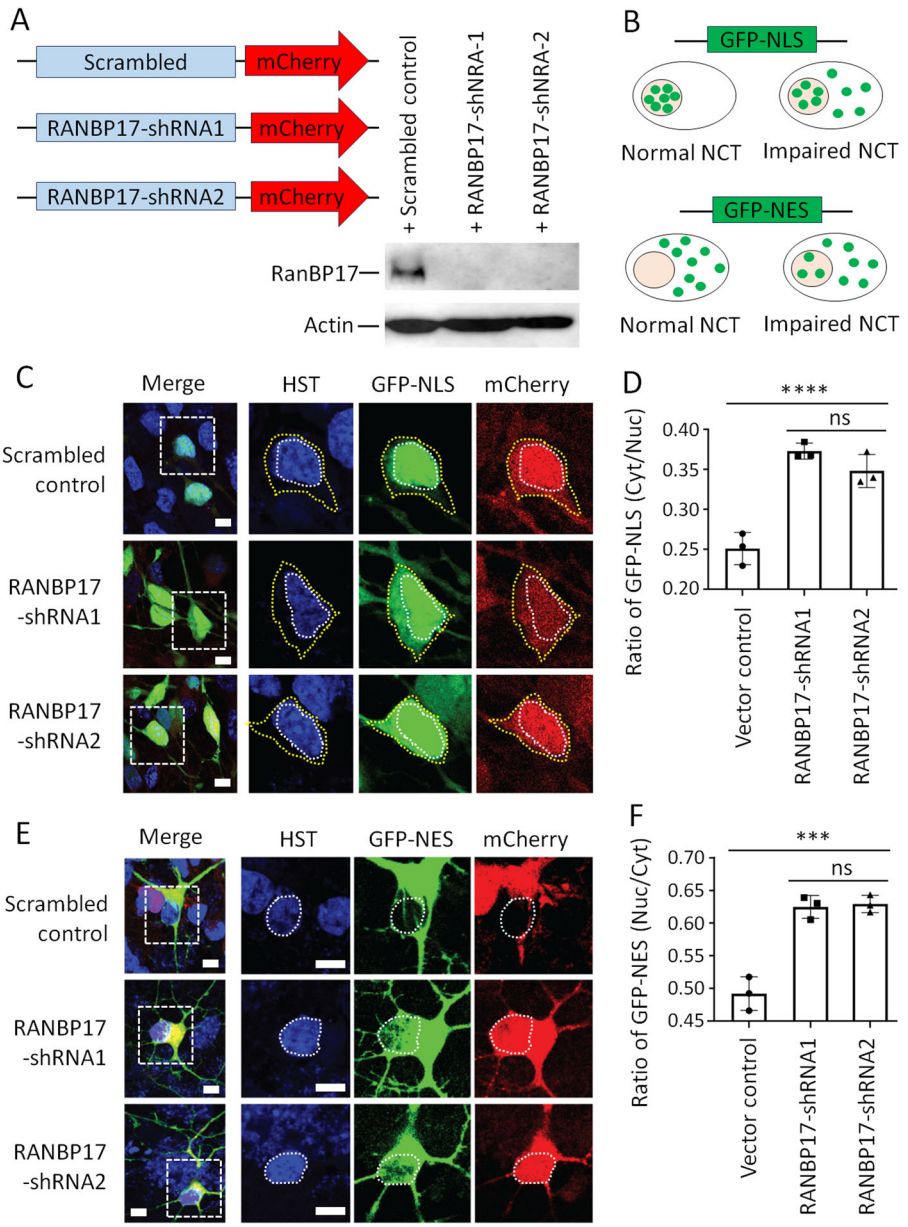


**Figure 4.** Downregulation of RANBP17 disrupts protein import and export in induced human MNs. ***A***, Construction and validation of lentiviral vectors expressing RANBP17-shRNAs. The vector contains the mCherry reporter. gRNA of scrambled sequencing serves as a control. ***B***, Schematic shows the constructions of lentiviral vectors expressing reporters GFP-NLS and GFP-NES and their expected subcellular distribution under normal and impaired NCT conditions. ***C***, Representative confocal images of MNs at 21 d postviral infection (dpi) coexpressed GFP-NLS and shRNA-mCherry. The nuclei and the soma were highlighted with white and yellow dotted lines, respectively. Scale bar, 20 µm. ***D***, The distribution of GFP-NLS reporter shown as a ratio of cytoplasmic to nuclear signal. *N* (neurons) = 178 for control, 162 for shRNA1, and 181 for shNRA2 from three independent experiments. ns, no significant difference; ****$p < 0.0001$. Student's *t* tests. ***E***, Representative confocal images of MNs at 21 dpi coexpressed GFP-NES and shRNA-mCherry. The nuclei were highlighted with dotted lines. Scale bar, 20 µm. ***F***, The distribution of GFP-NES reporter shown as a ratio of nuclear to cytoplasmic signal. *N* (neurons) = 142 for control, 133 for shRNA1, and 148 for shNRA2 from three independent experiments. ns, no significant difference; ***$p < 0.001$. Student's *t* tests.

### Restoring the impaired NCT in DYT1 MNs through overexpression of RANBP17

Previously, we demonstrated that the NCT activity was dysregulated in DYT1 patient–derived MNs (Ding et al., 2021). Currently, we further found that the expression of RANBP17 dramatically decreased in DYT1 MNs, and the downregulation of RANBP17 substantially hindered nuclear transport in healthy MNs. We postulated that the impaired NCT activity in DYT1 neurons is, at least in part, attributable to decreased RANBP17 levels. Furthermore, we hypothesized that overexpressing RANBP17 could rescue NCT activities and improve cellular functions in DYT1 neurons. Consequently, we developed lentiviral vectors for the ectopic expression of GFP-tagged RANBP17 (RANBP17-GFP), with a vector expressing GFP alone serving as a control. Western blot analysis validated the expression of both GFP and RANBP17-GFP at the anticipated sizes (Fig. 7*A*). To evaluate protein transport activities in DYT1 iPSC–derived MNs with overexpressed GFP or RANBP17-GFP, we employed RFP-NLS and RFP-NES reporters (Fig. 7*B*).

In DYT1 MNs expressing the GFP control, conspicuous RFP-NLS signals were detected in the cytoplasm, suggesting

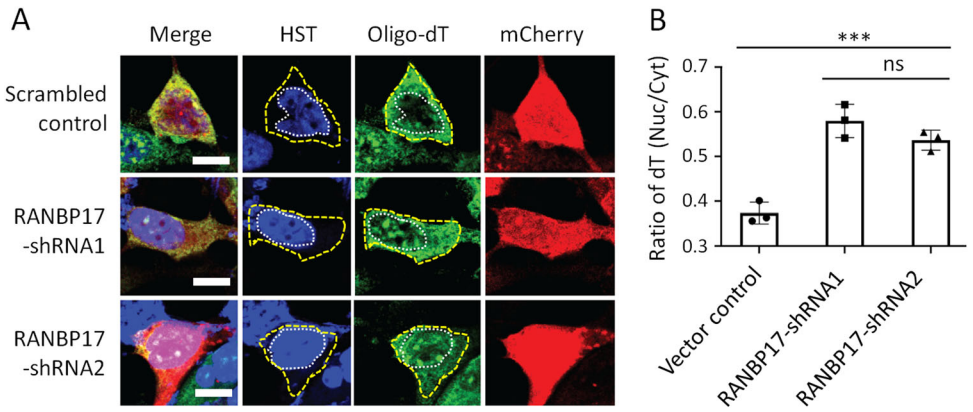


**Figure 5.** Downregulation of RANBP17 disrupts nuclear mRNA export. ***A***, Representative confocal images of FISH in iPSC-derived MNs at 21 dpi expressing RANBP17-shRNAs (mCherry positive). The nuclei and the soma were highlighted with white and yellow dotted lines, respectively. Scale bar, 20 µm. ***B***, The quantification data of mRNA distribution in ***A*** is shown as a ratio of nuclear to cytoplasmic oligo-dT signal. *N* (neurons) = 97 for control, 72 for shRNA1, and 78 for shRNA2 from three independent experiments. ns, no significant difference; ***$p < 0.001$. Student's *t* tests.

the compromised protein import. In contrast, DYT1 MNs expressing RANBP17-GFP exhibited significantly fewer cytoplasmic RFP-NLS signals (Fig. 7*C*). Likewise, utilizing the RFP-NES reporter, RANBP17 overexpression led to a marked reduction of nuclear RFP-NES in DYT1 MNs compared with the GFP controls (Fig. 7*D*). The ratios of cytoplasmic to nuclear RFP-NLS and nuclear to cytoplasmic RFP-NES were both notably diminished in DYT1 MNs with RANBP17 overexpression (Fig. 7*E,F*). These observations collectively indicate that the disrupted protein nuclear transport in DYT1 MNs can be reinstated by overexpression of RANBP17.

We also measured nuclear mRNA export using a FISH assay and found that RANBP17 overexpression partially rescued the impaired mRNA export in DYT1 MNs (Fig. 7*G*). Therefore, restoration of RANBP17 levels in DYT1 MNs can rescue the NCT activity of both protein and transcript cargos. Interestingly, we did not observe significant effects of RANBP17 overexpression on NCT activities in healthy MNs (Fig. 7*E–G*). This suggests that the endogenous level of RANBP17 is sufficient to maintain the efficient NCT functions in healthy MNs, or some functional cooperations with other RANBPs are needed to achieve its full activity.

### Overexpression of RANBP17 ameliorates neurite outgrowth and neuron maturation in DYT1 MNs

DYT1 is recognized as a neurodevelopmental disorder, with disrupted neurodevelopment observed in both mouse models and in vitro cultured DYT1 neurons (Tanabe et al., 2016; Ding et al., 2021; di Biase et al., 2022). We were wondering whether the rescued NCT, achieved through the restoration of RANBP17 expression levels in DYT1 neurons, could mitigate the compromised neurodevelopment. To this end, we assessed the neurite outgrowth and quantified branches of iPSC-MNs at different development stages. As expected, DYT1 MNs displayed shorter neurite lengths and significantly fewer primary (Fig. 8*B*) and secondary branches (Fig. 8*C*) in comparison with healthy controls. Remarkably, overexpressing RANBP17, but not the GFP control, substantially reinstated neurite outgrowth and the number of branches (Fig. 8*A–D*). Notably, the number of primary branches was nearly fully restored (Fig. 8*A*), while the number of secondary branches and neurite length exhibited partial restoration (Fig. 8*C,D*). To further examine the impact of RANBP17 overexpression on DYT1 neuron maturation, we analyzed the expression of genes involved in neuron maturation using RT-PCR. Compared with GFP controls, overexpression of RANBP17 in DYT1 iMNs showed a significant increase in the expressions of SYN1, VGLUT1, and VGLUT2 at both time points of 14 and 21 dpi. NeuN expression only exhibited a slight increase at 14 dpi, with no significant difference at 21 dpi (Fig. 8*E*). These results demonstrate that restoration of RANBP17 level ameliorates the neurite outgrowth and neuron maturation in DYT1 MNs.

## Discussion

DYT1 dystonia is a hereditary neurological movement disorder characterized by involuntary muscle contractions, which lead to repetitive and often twisting movements or abnormal postures (Balint et al., 2018). The condition typically manifests during adolescence or early adulthood and can result in varying degrees of impairment in daily activities (Dauer, 2014; Li et al., 2021). However, the anatomical basis for DYT1 dystonia remains a topic of ongoing debate (Di Fonzo et al., 2022; Morigaki and Miyamoto, 2022). Historically, dystonia has been conceptualized as a disorder originating in the basal ganglia (Ip et al., 2016; Maltese et al., 2018), subcortical nuclei involved in diverse functions including motor control and motor learning (Downs et al., 2019). Subsequent investigations have proposed that dystonia should be understood as a network disorder, involving the basal ganglia–cerebello-thalamo-cortical circuit (Egger et al., 2007; Jinnah et al., 2017; Balint et al., 2018; Maltese et al., 2018; Bai et al., 2021; Nieuwhof et al., 2022). Recent reports have also pointed toward the cerebellum (Fremont et al., 2017; Tewari et al., 2017) and the spinal cord (Zhang et al., 2017; Pocratsky et al., 2023) as potential major sites of dysfunction in *Tor1a* knock-out mice.

Currently, the majority of research on dystonia relies on patient postmortem tissues or rodent models (Balint et al., 2018; Bai et al., 2021). However, certain changes within brain tissues may be transient, making their preservation and detection in posthumous tissues challenging (Augood et al., 2003). While animal models offer insights into disease mechanisms, substantial differences based on species are present, and these models only capture limited aspects of human dystonia's pathophysiology. For example, mice carrying the heterozygous mutation (ΔE) identical to that found in DYT1 patients do not display

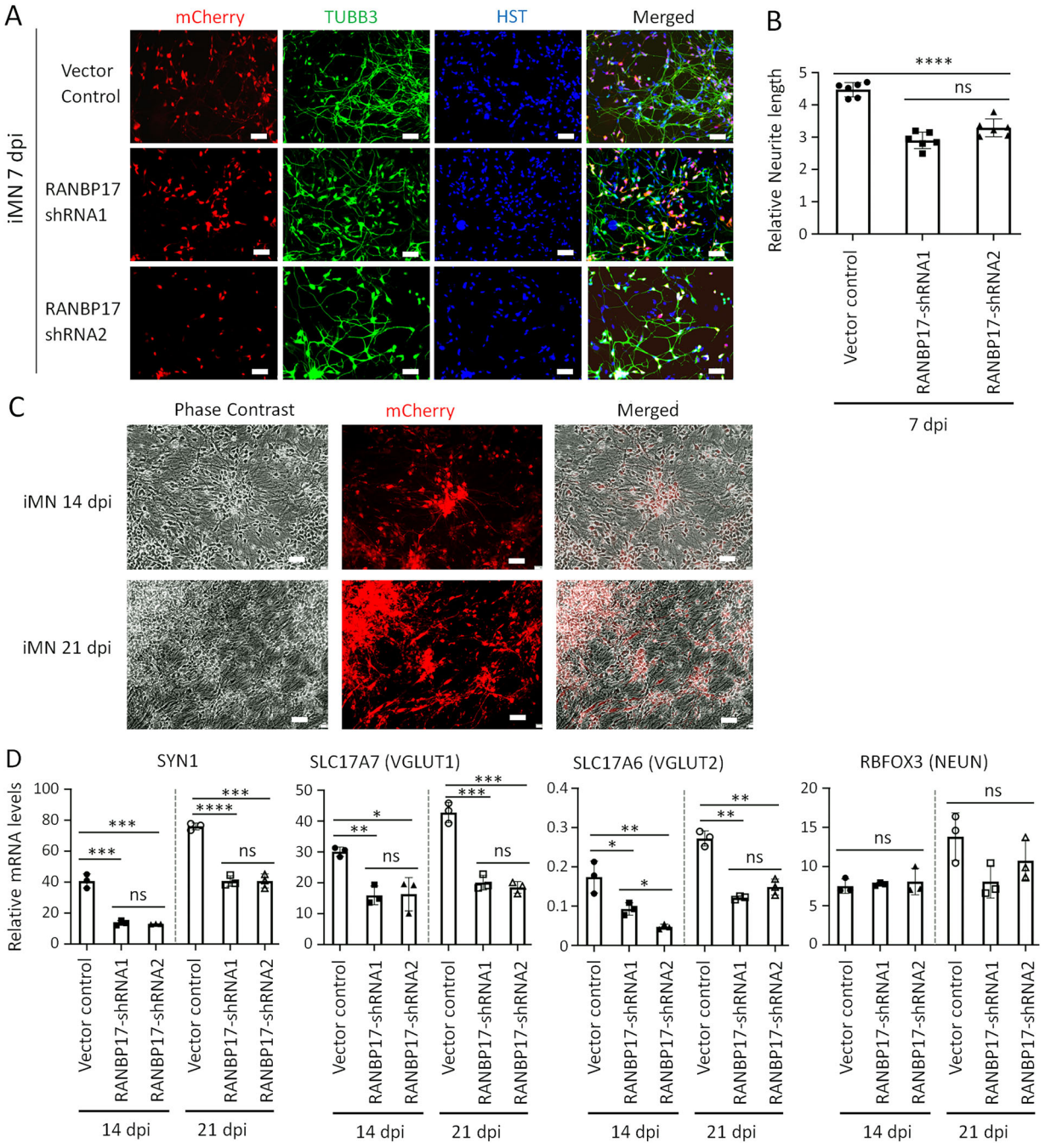


**Figure 6.** Downregulation of RANBP17 disrupts neurite outgrowth and neuron maturation. ***A***, Representative micrographs of healthy iMNs transduced with indicated shRNAs (mCherry +) at 7 dpi. Scale bar, 50 µm. ***B***, Quantification of neurite outgrowth of healthy iMNs at 7 dpi infected with lentivirus expressing RANBP17-shRNAs. *N* (neurons) = 192 for control, 203 for shRNA1, and 187 for shRNA2 from six independent experiments. ns, no significant difference; $****p < 0.0001$. Student's *t* tests. ***C***, Representative micrographs of healthy iMNs transduced with lentivirus expressing RANBP17-shRNAs at 14 and 21 dpi when collecting RNA samples for gene expression assay. Scale bar, 50 µm. ***D***, RT-PCR assay of genes related to neuron maturation in RNA samples from ***C***. *N*, three independent experiments. ns, no significant difference; $*p < 0.05$; $**p < 0.01$; $***p < 0.001$; $****p < 0.0001$. Student's *t* tests.

noticeable pathology (Goodchild et al., 2005; Gonzalez-Alegre, 2019). Furthermore, utilizing posthumous tissues or rodent models poses difficulties in deciphering the molecular underpinnings through biochemical approaches, which typically demand a substantial number of high-purity living neurons.

In the present study, we conducted a transcriptomic analysis to identify dysregulated genes in DYT1 patient–derived MNs. To the best of our knowledge, this marks the initial investigation into comprehensive changes in gene expression across the genome within human DYT1 dystonia neurons. Our findings reveal that dysregulated genes in human DYT1 MNs play substantial roles in neurodevelopment and various BPs, thereby offering fresh perspectives on the underlying mechanisms of DYT1 dystonia's pathophysiology. Furthermore, we identified that the reduced RANBP17 levels contribute to the impairment of NCT in DYT1 neurons, a prominent cellular deficiency we previously discovered (Ding et al., 2021). Most importantly, the overexpression of RANBP17 emerged as a substantial mitigating factor, effectively restoring impaired NCT activity and rescuing neurodevelopmental deficits observed in DYT1 MNs. These findings

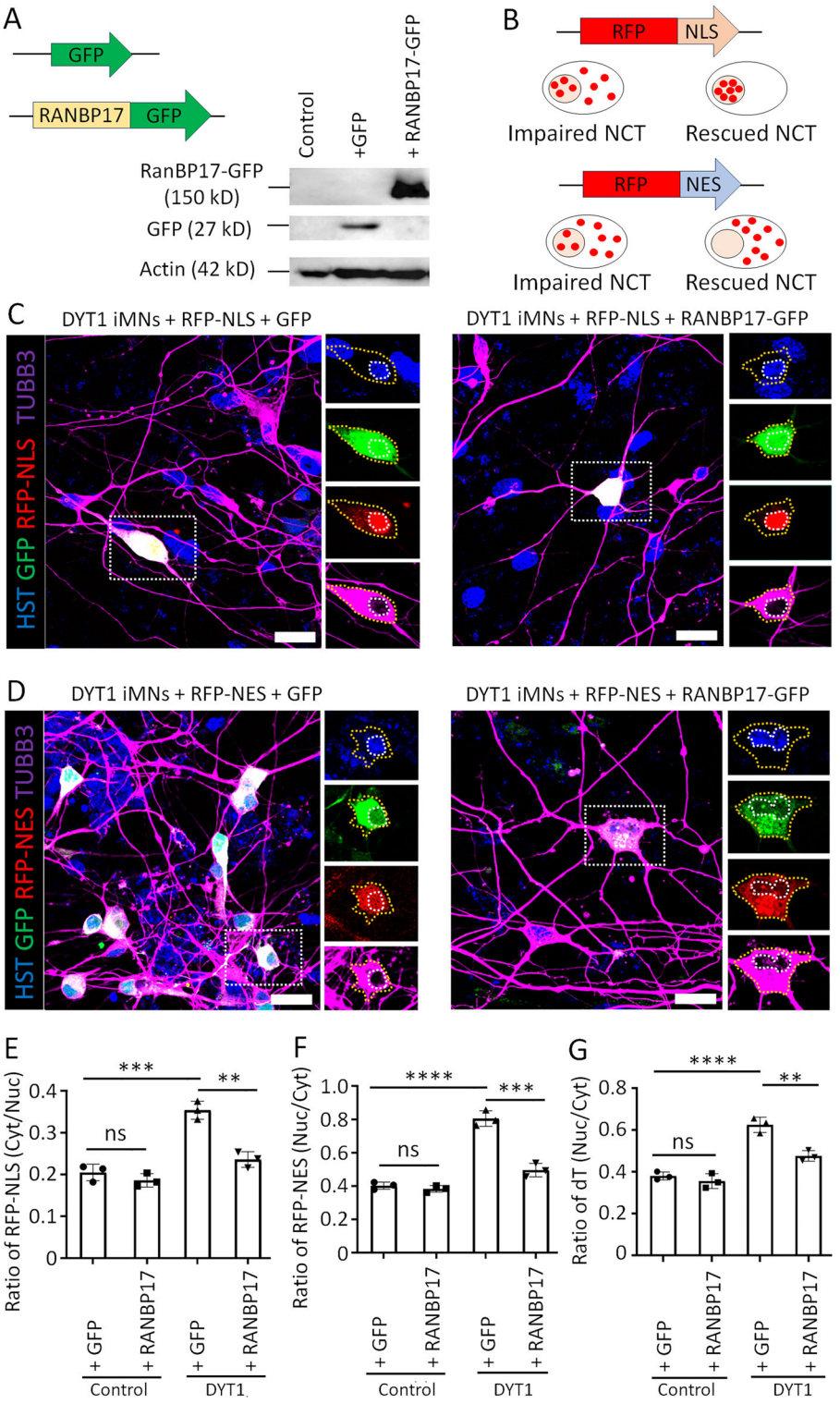


**Figure 7.** Overexpression of RANBP17 ameliorates the impaired NCT in DYT1 MNs. ***A***, Construction and validation of lentiviral vectors expressing GFP-tagged RANBP17 and GFP alone. ***B***, Schematic shows the constructions of lentiviral vectors expressing transport reporters RFP-NLS and RFP-NES and the expected subcellular distribution under normal and impaired NCT conditions. ***C***, Representative confocal images of DYT1 MNs at 21 dpi coexpressed RFP-NLS and GFP or RANBP17-GFP. The nuclei and the soma were highlighted with white and yellow dotted lines, respectively. Scale bar, 50 µm. ***D***, Representative confocal images of DYT1 MNs at 21 dpi coexpressed RFP-NES and GFP or RANBP17-GFP. The nuclei and the soma were highlighted with white and yellow dotted lines, respectively. Scale bar, 50 µm. ***E***, The distribution of RFP-NLS signal under indicated conditions is shown as a ratio of cytoplasmic to nuclear signal. *N* (neurons) = 120 for health + GFP, 113 for health + RANBP17, 95 for DYT1 + GFP, and 97 for DYT1 + RANBP17 from three independent experiments. ns, no significant difference; $^{**}p < 0.01$; $^{***}p < 0.001$. Student's *t* tests. ***F***, The distribution of RFP-NES signal under indicated conditions is shown as a ratio of nuclear to cytoplasmic signal. *N* (neurons) = 122 for health + GFP, 113 for health + RANBP17, 125 for DYT1 + GFP, and 121 for DYT1 + RANBP17 from three independent experiments. ns, no significant difference; $^{***}p < 0.001$, $^{****}p < 0.0001$. Student's *t* tests. ***G***, The quantification data of FISH assay shown as a ratio of nuclear to cytoplasmic oligo-dT signal. *N* (neurons) = 104 for health + GFP, 97 for health + RANBP17, 95 for DYT1 + GFP, and 89 for DYT1 + RANBP17 from three independent experiments. ns, no significant difference; $^{**}p < 0.01$, $^{****}p < 0.0001$. Student's *t* tests.

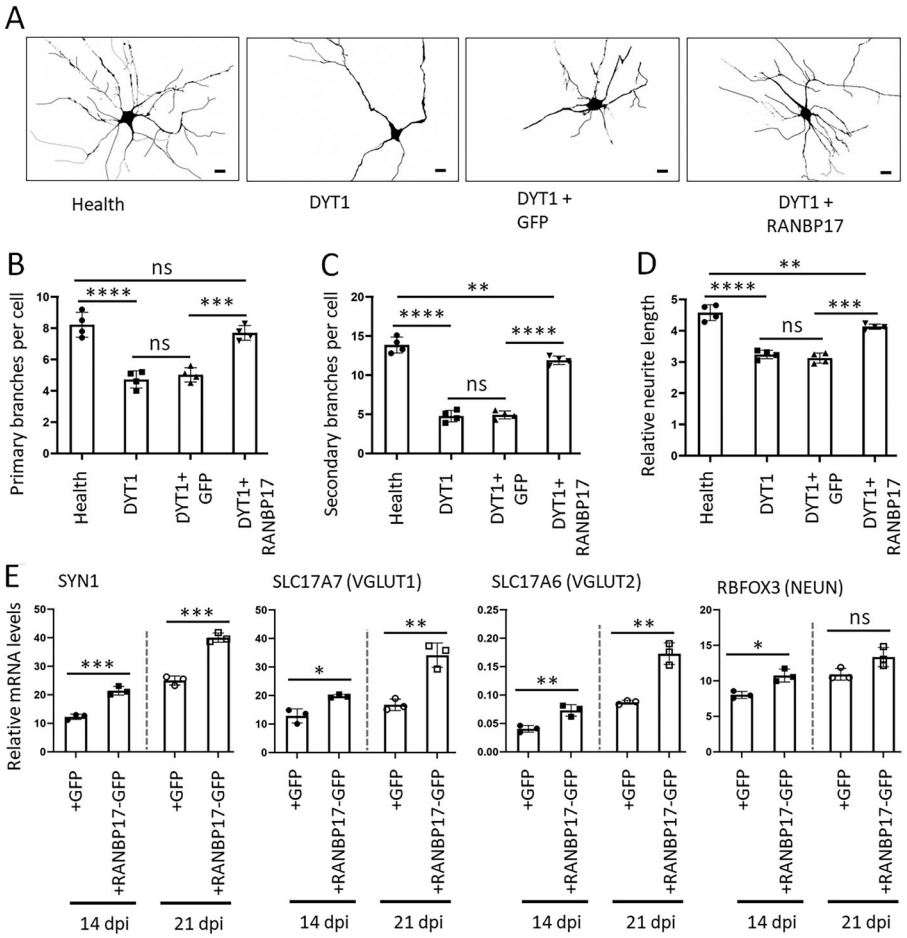


**Figure 8.** Overexpression of RANBP17 ameliorates neurite outgrowth and neuron maturation in DYT1 neurons. ***A***, Representative images of iMNs under indicated conditions at 21 dpi. The morphology was based on the ICC of TUBB3. Scale bar, 50 µm. ***B***, The number of primary branches of iMNs at 21 dpi under indicated conditions. ***C***, The number of secondary branches of iMNs at 21 dpi under indicated conditions. For ***B*** and ***C***, *N* (neurons) = 57 for health, 52 for DYT1, 48 for DYT1 + GFP, and 53 for DYT1 + RANBP17 from four independent experiments. ns, no significant difference; $^{**}p < 0.01$; $^{***}p < 0.001$, $^{****}p < 0.0001$. Student's *t* tests. ***D***, The relative neurite length of iMNs at 14 dpi under indicated conditions. *N* (neurons) = 127 for health, 112 for DYT1, 94 for DYT1 + GFP, and 93 for DYT1 + RANBP17 from four independent experiments. ns, no significant difference; $^{**}p < 0.01$; $^{***}p < 0.001$, $^{****}p < 0.0001$. Student's *t* tests. ***E***, RT-PCR assay of genes related to neuron maturation in DYT1 iMNs with overexpression of RANBP17-GFP and GFP control at 14 and 21 dpi. *N*, three independent experiments. ns, no significant difference; $^{*}p < 0.05$; $^{**}p < 0.01$; $^{***}p < 0.001$. Student's *t* tests.

shed light on the intricate molecular underpinnings of impaired NCT in DYT1 neurons and hold potential for developing innovative treatment strategies.

In the NCT regulation, members of the importin-β family can either independently bind and transport cargo from the cytoplasm to the nucleus, or they can create heterodimers with importin-α. Within this heterodimer structure, importin-β facilitates interactions with the NPC, while importin-α serves as an adaptor protein, binding to the NLS on the cargo (Mattaj and Englmeier, 1998; Adam, 1999; Wing et al., 2022). Despite RANBP17's identification as a member of the importin-β superfamily over two decades ago (Kutay et al., 2000), there has been limited involvement of RANBP17 in research, as indicated by a search on PubMed. Although a few studies have revealed RANBP17's association with the activation of bHLH transcription factors (Lee et al., 2010) and the involvement in aging biology (Mertens et al., 2015), as well as its role in promoting cancer cell proliferation (Mandic et al., 2022), the precise functions of RANBP17 in NCT regulation and the underlying molecular mechanisms remain to be delineated.

In this study, using transport reporters and FISH assay together with the manipulation of RANBP17 by shRNAs, we demonstrated that RANBP17 plays a crucial role in protein import, which is consistent with its classification as a member of the importin-β superfamily. Interestingly, we also observed that the downregulation of RANBP17 also compromised the protein and mRNA export activities in induced human neurons. This could be due to the reciprocal influence on each other between the import and export pathways. Specifically, the impairment of protein import disrupts critical factors for nuclear exporting pathways, including the disturbance of the RAN cycle and the failure to import exportins into the nucleus, culminating in both compromised importing and exporting activities. Notably, this study represents the first comprehensive assessment of RANBP17's roles in both nuclear import and export of protein and mRNA cargos, offering the molecular underpinnings for understanding the dysregulation of RANBP17 under various diseased conditions (Mertens et al., 2015; Mandic et al., 2022). Furthermore, the overexpression of RANBP17 effectively mitigates the neurodevelopmental deficits observed in DYT1 MNs, thereby furnishing new evidence for the pivotal role of NCT activities in neurodevelopment and neuron maturation. Consequently, manipulating NCT activities could offer innovative treatment strategies for neurodevelopmental disorders.

An interesting question that needs to be addressed is how the ΔE mutation causes the reduced expression of RANBP17. Presentably, we lack direct evidence to conclusively address this question. However, considering that the distorted nucleus is a prevalent cellular characteristic in DYT1 cells (Ding et al., 2021), we propose that the reorganization of chromatin structure prompted by nuclear deformation might contribute to alterations in the expression of multiple genes, including RANBP17 (Neelam et al., 2020; Chi et al., 2022). Further investigation is imperative to gain a comprehensive understanding of the intricate mechanisms responsible for the dysregulation of RANBP17 in the context of DYT1 dystonia.

Our study has provided compelling evidence that the diminished RANBP17 levels contribute to the impaired NCT activities observed in DYT1 neurons, while the overexpression of RANBP17 efficiently reinstates NCT activity and rescues neurodevelopmental deficits in DYT1 neurons. Nevertheless, we acknowledge certain limitations in our investigation and analysis. Firstly, our exploration into the genome-wide changes of gene expression in human DYT1 dystonia neurons remains preliminary. While we have identified numerous dysregulated genes in DYT1 neurons, delving into the molecular mechanisms underpinning their dysregulation and their contributions to the pathophysiology of DYT1 dystonia requires further probing. Secondly, despite our extensive investigation into the roles of RANBP17 in regulating nuclear transport and its impact on neuronal development and maturation, further electrophysiology analysis is necessary to confirm any changes in neuronal function. Thirdly, we recognize that our findings stem from an in vitro cellular system. To establish their clinical relevance, we require a thorough investigation utilizing brain tissues from DYT1 patients. In this vein, we have already obtained such samples, with ongoing analysis in a separate project poised to offer invaluable insights into the clinical significance of our findings.

## References


Adam SA (1999) Transport pathways of macromolecules between the nucleus and the cytoplasm. Curr Opin Cell Biol 11:402–406.

Akter M, Cui H, Chen YH, Ding B (2021) Generation of two induced pluripotent stem cell lines with heterozygous and homozygous GAG deletion in TOR1A gene from a healthy hiPSC line. Stem Cell Res 56:102536.

Akter M, Cui H, Chen YH, Ding B (2022a) Generation of gene-corrected isogenic control cell lines from a DYT1 dystonia patient iPSC line carrying a heterozygous GAG mutation in TOR1A gene. Stem Cell Res 62:102807.

Akter M, Cui H, Sepehrimanesh M, Hosain MA, Ding B (2022b) Generation of highly pure motor neurons from human induced pluripotent stem cells. STAR Protoc 3:101223.

Akter M, Ding B (2022) Modeling movement disorders via generation of hiPSC-derived motor neurons. Cells 11:3796.

Anders S, Huber W (2010) Differential expression analysis for sequence count data. Genome Biol 11:R106.

Andreu I, et al. (2022) Mechanical force application to the nucleus regulates nucleocytoplasmic transport. Nat Cell Biol 24:896–905.

Augood SJ, Keller-McGandy CE, Siriani A, Hewett J, Ramesh V, Sapp E, DiFiglia M, Breakefield XO, Standaert DG (2003) Distribution and ultrastructural localization of torsinA immunoreactivity in the human brain. Brain Res 986:12–21.

Bai X, Vajkoczy P, Faust K (2021) Morphological abnormalities in the basal ganglia of dystonia patients. Stereotact Funct Neurosurg 99:351–362.

Balint B, Mencacci NE, Valente EM, Pisani A, Rothwell J, Jankovic J, Vidailhet M, Bhatia KP (2018) Dystonia. Nat Rev Dis Primers 4:25.

Barbato S, Kapinos LE, Rencurel C, Lim RYH (2020) Karyopherin enrichment at the nuclear pore complex attenuates Ran permeability. J Cell Sci 133:jcs238121.

Becskei A, Mattaj IW (2003) The strategy for coupling the RanGTP gradient to nuclear protein export. Proc Natl Acad Sci U S A 100:1717–1722.

Burk K, Pasterkamp RJ (2019) Disrupted neuronal trafficking in amyotrophic lateral sclerosis. Acta Neuropathol 137:859–877.

Charlesworth G, Bhatia KP, Wood NW (2013) The genetics of dystonia: new twists in an old tale. Brain 136:2017–2037.

Chen V, Moncalvo M, Tringali D, Tagliaferro L, Shriskanda A, Ilich E, Dong W, Kantor B, Chiba-Falek O (2020) The mechanistic role of α-synuclein in the nucleus: impaired nuclear function caused by familial Parkinson's disease SNCA mutations. Hum Mol Genet 29:3107–3121.

Cheng L, et al. (2004) Tlx3 and Tlx1 are post-mitotic selector genes determining glutamatergic over GABAergic cell fates. Nat Neurosci 7:510–517.

Chi YH, Wang WP, Hung MC, Liou GG, Wang JY, Chao PG (2022) Deformation of the nucleus by TGFbeta1 via the remodeling of nuclear envelope and histone isoforms. Epigenetics Chromatin 15:1.

Chou CC, et al. (2018) TDP-43 pathology disrupts nuclear pore complexes and nucleocytoplasmic transport in ALS/FTD. Nature Neuroscience 21: 228–239.

Cui H, Sepehrimanesh M, Coutee C, Akter M, Hosain A, Ding B (2022) Protocol to image and quantify nucleocytoplasmic transport in cultured cells using fluorescent in situ hybridization and a dual reporter system. STAR Protoc 3:101813.

Dauer W (2014) Inherited isolated dystonia: clinical genetics and gene function. Neurotherapeutics 11:807–816.

Delphin C, Guan T, Melchior F, Gerace L (1997) RanGTP targets p97 to RanBP2, a filamentous protein localized at the cytoplasmic periphery of the nuclear pore complex. Mol Biol Cell 8:2379–2390.

di Biase L, Di Santo A, Caminiti ML, Pecoraro PM, Di Lazzaro V (2022) Classification of dystonia. Life 12:206.

Di Fonzo A, Albanese A, Jinnah HA (2022) The apparent paradox of phenotypic diversity and shared mechanisms across dystonia syndromes. Curr Opin Neurol 35:502–509.

Ding B (2015) Gene expression in maturing neurons: regulatory mechanisms and related neurodevelopmental disorders. Sheng Li Xue Bao 67:113–133.

Ding B (2021) Generation of patient-specific motor neurons in modeling movement diseases. Neural Regen Res 16:1799–1800.

Ding B (2022) Novel insights into the pathogenesis of DYT1 dystonia from induced patient-derived neurons. Neural Regen Res 17:561–562.

Ding B, Akter M, Zhang CL (2020) Differential influence of sample sex and neuronal maturation on mRNA and protein transport in induced human neurons. Front Mol Neurosci 13:46.

Ding B, Cave JW, Dobner PR, Mullikin-Kilpatrick D, Bartzokis M, Zhu H, Chow CW, Gronostajski RM, Kilpatrick DL (2016) Reciprocal autoregulation by NFI occupancy and ETV1 promotes the developmental expression of dendrite-synapse genes in cerebellar granule neurons. Mol Biol Cell 27:1488–1499.

Ding B, Dobner PR, Mullikin-Kilpatrick D, Wang W, Zhu H, Chow CW, Cave JW, Gronostajski RM, Kilpatrick DL (2018) BDNF activates an NFI-dependent neurodevelopmental timing program by sequestering NFATc4. Mol Biol Cell 29:975–987.

Ding B, Kilpatrick DL (2013) Lentiviral vector production, titration, and transduction of primary neurons. Methods Mol Biol 1018:119–131.

Ding B, LeJeune D, Li S (2010) The C-terminal repeat domain of Spt5 plays an important role in suppression of Rad26-independent transcription coupled repair. J Biol Chem 285:5317–5326.

Ding B, Sepehrimanesh M (2021) Nucleocytoplasmic transport: regulatory mechanisms and the implications in neurodegeneration. Int J Mol Sci 22:4165.

Ding B, Tang Y, Ma S, Akter M, Liu ML, Zang T, Zhang CL (2021) Disease modeling with human neurons reveals LMNB1 dysregulation underlying DYT1 dystonia. J Neurosci 41:2024–2038.

Ding B, Wang W, Selvakumar T, Xi HS, Zhu H, Chow CW, Horton JD, Gronostajski RM, Kilpatrick DL (2013) Temporal regulation of nuclear factor one occupancy by calcineurin/NFAT governs a voltage-sensitive developmental switch in late maturing neurons. J Neurosci 33: 2860–2872.

Downs AM, Roman KM, Campbell SA, Pisani A, Hess EJ, Bonsi P (2019) The neurobiological basis for novel experimental therapeutics in dystonia. Neurobiol Dis 130:104526.

Duan W, Zhang YP, Hou Z, Huang C, Zhu H, Zhang CQ, Yin Q (2016) Novel insights into NeuN: from neuronal marker to splicing regulator. Mol Neurobiol 53:1637–1647.

Dull T, Zufferey R, Kelly M, Mandel RJ, Nguyen M, Trono D, Naldini L (1998) A third-generation lentivirus vector with a conditional packaging system. J Virol 72:8463–8471.

Duverger O, Morasso MI (2008) Role of homeobox genes in the patterning, specification, and differentiation of ectodermal appendages in mammals. J Cell Physiol 216:337–346.
Eftekharzadeh B, et al. (2018) Tau protein disrupts nucleocytoplasmic transport in Alzheimer's disease. Neuron 99:925–940 e927.
Egger K, Mueller J, Schocke M, Brenneis C, Rinnerthaler M, Seppi K, Trieb T, Wenning GK, Hallett M, Poewe W (2007) Voxel based morphometry reveals specific gray matter changes in primary dystonia. Mov Disord 22:1538–1542.
El Mestikawy S, Wallen-Mackenzie A, Fortin GM, Descarries L, Trudeau LE (2011) From glutamate co-release to vesicular synergy: vesicular glutamate transporters. Nat Rev Neurosci 12:204–216.
Freibaum BD, et al. (2015) GGGGCC repeat expansion in C9orf72 compromises nucleocytoplasmic transport. Nature 525:129–133.
Fremont R, Tewari A, Angueyra C, Khodakhah K (2017) A role for cerebellum in the hereditary dystonia DYT1. Elife 6:22775.
Fung HYJ, Chook YM (2022) Binding affinity measurement of nuclear export signal peptides to their exporter CRM1. Methods Mol Biol 2502:245–256.
Gasset-Rosa F, Chillon-Marinas C, Goginashvili A, Atwal RS, Artates JW, Tabet R, Wheeler VC, Bang AG, Cleveland DW, Lagier-Tourenne C (2017) Polyglutamine-expanded huntingtin exacerbates age-related disruption of nuclear integrity and nucleocytoplasmic transport. Neuron 94:48–57 e44.
Gonzalez-Alegre P (2019) Advances in molecular and cell biology of dystonia: focus on torsinA. Neurobiol Dis 127:233–241.
Goodchild RE, Kim CE, Dauer WT (2005) Loss of the dystonia-associated protein torsinA selectively disrupts the neuronal nuclear envelope. Neuron 48:923–932.
Gorlich D, Dabrowski M, Bischoff FR, Kutay U, Bork P, Hartmann E, Prehn S, Izaurralde E (1997) A novel class of RanGTP binding proteins. J Cell Biol 138:65–80.
Grima JC, et al. (2017) Mutant huntingtin disrupts the nuclear pore complex. Neuron 94:93–107 e106.
Grunwald D, Singer RH, Rout M (2011) Nuclear export dynamics of RNA-protein complexes. Nature 475:333–341.
Guo Z, et al. (2012) Tlx1/3 and Ptf1a control the expression of distinct sets of transmitter and peptide receptor genes in the developing dorsal spinal cord. J Neurosci 32:8509–8520.
Hanson PI, Whiteheart SW (2005) AAA+ proteins: have engine, will work. Nat Rev Mol Cell Biol 6:519–529.
Hetzer MW (2010) The nuclear envelope. Cold Spring Harb Perspect Biol 2: a000539.
Ip CW, et al. (2016) Tor1a+/- mice develop dystonia-like movements via a striatal dopaminergic dysregulation triggered by peripheral nerve injury. Acta Neuropathol Commun 4:108.
Jinnah HA, Neychev V, Hess EJ (2017) The anatomical basis for dystonia: the motor network model. Tremor Other Hyperkinet Mov (N Y) 7:506.
Jokhi V, Ashley J, Nunnari J, Noma A, Ito N, Wakabayashi-Ito N, Moore MJ, Budnik V (2013) Torsin mediates primary envelopment of large ribonucleoprotein granules at the nuclear envelope. Cell Rep 3:988–995.
Jovicic A, et al. (2015) Modifiers of C9orf72 dipeptide repeat toxicity connect nucleocytoplasmic transport defects to FTD/ALS. Nat Neurosci 18:1226–1229.
Kalita J, Kapinos LE, Lim RYH (2021) On the asymmetric partitioning of nucleocytoplasmic transport - recent insights and open questions. J Cell Sci 134:jcs240382.
Keller Sarmiento IJ, Mencacci NE (2021) Genetic dystonias: update on classification and new genetic discoveries. Curr Neurol Neurosci Rep 21:8.
Kerrisk ME, Cingolani LA, Koleske AJ (2014) ECM receptors in neuronal structure, synaptic plasticity, and behavior. Prog Brain Res 214:101–131.
Kim HJ, Taylor JP (2017) Lost in transportation: nucleocytoplasmic transport defects in ALS and other neurodegenerative diseases. Neuron 96:285–297.
Kopito RB, Elbaum M (2007) Reversibility in nucleocytoplasmic transport. Proc Natl Acad Sci U S A 104:12743–12748.
Kutay U, Hartmann E, Treichel N, Calado A, Carmo-Fonseca M, Prehn S, Kraft R, Gorlich D, Bischoff FR (2000) Identification of two novel RanGTP-binding proteins belonging to the importin beta superfamily. J Biol Chem 275:40163–40168.
Lange A, Mills RE, Lange CJ, Stewart M, Devine SE, Corbett AH (2007) Classical nuclear localization signals: definition, function, and interaction with importin alpha. J Biol Chem 282:5101–5105.
Laudermilch E, Schlieker C (2016) Torsin ATPases: structural insights and functional perspectives. Curr Opin Cell Biol 40:1–7.
Laudermilch E, Tsai PL, Graham M, Turner E, Zhao C, Schlieker C (2016) Dissecting Torsin/cofactor function at the nuclear envelope: a genetic study. Mol Biol Cell 27:3964–3971.
Lee JH, Zhou S, Smas CM (2010) Identification of RANBP16 and RANBP17 as novel interaction partners for the bHLH transcription factor E12. J Cell Biochem 111:195–206.
Lester E, Parker R (2018) The tau of nuclear-cytoplasmic transport. Neuron 99:869–871.
Li J, Levin DS, Kim AJ, Pappas SS, Dauer WT (2021) Torsina restoration in a mouse model identifies a critical therapeutic window for DYT1 dystonia. J Clin Invest 131:e139606.
Lim Y (2023) Transcription factors in microcephaly. Front Neurosci 17: 1302033.
Mahajan R, Delphin C, Guan T, Gerace L, Melchior F (1997) A small ubiquitin-related polypeptide involved in targeting RanGAP1 to nuclear pore complex protein RanBP2. Cell 88:97–107.
Maltese M, et al. (2018) Early structural and functional plasticity alterations in a susceptibility period of DYT1 dystonia mouse striatum. Elife 7:e33331.
Mandic R, et al. (2022) The importin beta superfamily member RanBP17 exhibits a role in cell proliferation and is associated with improved survival of patients with HPV+ HNSCC. BMC Cancer 22:785.
Mattaj IW, Englmeier L (1998) Nucleocytoplasmic transport: the soluble phase. Annu Rev Biochem 67:265–306.
Melchior F, Guan T, Yokoyama N, Nishimoto T, Gerace L (1995) GTP hydrolysis by Ran occurs at the nuclear pore complex in an early step of protein import. J Cell Biol 131:571–581.
Mertens J, et al. (2015) Directly reprogrammed human neurons retain aging-associated transcriptomic signatures and reveal Age-related nucleocytoplasmic defects. Cell Stem Cell 17:705–718.
Moore MS, Blobel G (1993) The GTP-binding protein Ran/TC4 is required for protein import into the nucleus. Nature 365:661–663.
Morigaki R, Miyamoto R (2022) Dystonia: still a mysterious syndrome. Life 12:989.
Moroianu J, Blobel G (1995) Protein export from the nucleus requires the GTPase Ran and GTP hydrolysis. Proc Natl Acad Sci U S A 92:4318–4322.
Naismith TV, Dalal S, Hanson PI (2009) Interaction of torsinA with its major binding partners is impaired by the dystonia-associated DeltaGAG deletion. J Biol Chem 284:27866–27874.
Naismith TV, Heuser JE, Breakefield XO, Hanson PI (2004) Torsina in the nuclear envelope. Proc Natl Acad Sci U S A 101:7612–7617.
Neelam S, Richardson B, Barker R, Udave C, Gilroy S, Cameron MJ, Levine HG, Zhang Y (2020) Changes in nuclear shape and gene expression in response to simulated microgravity are LINC complex-dependent. Int J Mol Sci 21:6762.
Nieuwhof F, Toni I, Dirkx MF, Gallea C, Vidailhet M, Buijink AWG, van Rootselaar AF, van de Warrenburg BPC, Helmich RC (2022) Cerebello-thalamic activity drives an abnormal motor network into dystonic tremor. Neuroimage Clin 33:102919.
Ogura T, Wilkinson AJ (2001) AAA+ superfamily ATPases: common structure–diverse function. Genes Cells 6:575–597.
Ozelius LJ, et al. (1997) The early-onset torsion dystonia gene (DYT1) encodes an ATP-binding protein. Nat Genet 17:40–48.
Paci G, Zheng T, Caria J, Zilman A, Lemke EA (2020) Molecular determinants of large cargo transport into the nucleus. Elife 9:e55963.
Packard M, Jokhi V, Ding B, Ruiz-Canada C, Ashley J, Budnik V (2015) Nucleus to synapse nesprin1 railroad tracks direct synapse maturation through RNA localization. Neuron 86:1015–1028.
Pappas SS, Liang CC, Kim S, Rivera CO, Dauer WT (2018) Torsina dysfunction causes persistent neuronal nuclear pore defects. Hum Mol Genet 27: 407–420.
Park HS, Lee J, Lee HS, Ahn SH, Ryu HY (2022) Nuclear mRNA export and aging. Int J Mol Sci 23:5451.
Parra AS, Johnston CA (2022) Emerging roles of RNA-binding proteins in neurodevelopment. J Dev Biol 10:23.
Pelossof R, et al. (2017) Prediction of potent shRNAs with a sequential classification algorithm. Nat Biotechnol 35:350–353.
Pocratsky AM, Nascimento F, Ozyurt MG, White IJ, Sullivan R, O'Callaghan BJ, Smith CC, Surana S, Beato M, Brownstone RM (2023) Pathophysiology of Dyt1-Tor1a dystonia in mice is mediated by spinal neural circuit dysfunction. Sci Transl Med 15:eadg3904.
Rampello AJ, Prophet SM, Schlieker C (2020) The role of torsin AAA+ proteins in preserving nuclear envelope integrity and safeguarding against disease. Biomolecules 10:468.

Rittiner JE, et al. (2016) Functional genomic analyses of Mendelian and sporadic disease identify impaired eIF2alpha signaling as a generalizable mechanism for dystonia. Neuron 92:1238–1251.
Sansevrino R, Hoffmann C, Milovanovic D (2023) Condensate biology of synaptic vesicle clusters. Trends Neurosci 46:293–306.
Seewald MJ, Korner C, Wittinghofer A, Vetter IR (2002) RanGAP mediates GTP hydrolysis without an arginine finger. Nature 415:662–666.
Seewald MJ, Kraemer A, Farkasovsky M, Korner C, Wittinghofer A, Vetter IR (2003) Biochemical characterization of the Ran-RanBP1-RanGAP system: are RanBP proteins and the acidic tail of RanGAP required for the Ran-RanGAP GTPase reaction? Mol Cell Biol 23:8124–8136.
Sepehrimanesh M, Akter M, Ding B (2021) Direct conversion of adult fibroblasts into motor neurons. STAR Protoc 2:100917.
Sepehrimanesh M, Ding B (2020) Generation and optimization of highly pure motor neurons from human induced pluripotent stem cells via lentiviral delivery of transcription factors. Am J Physiol Cell Physiol 319:C771–C780.
Stewart M (2007) Molecular mechanism of the nuclear protein import cycle. Nat Rev Mol Cell Biol 8:195–208.
Tanabe LM, Liang CC, Dauer WT (2016) Neuronal nuclear membrane budding occurs during a developmental window modulated by torsin paralogs. Cell Rep 16:3322–3333.
Terry LJ, Wente SR (2009) Flexible gates: dynamic topologies and functions for FG nucleoporins in nucleocytoplasmic transport. Eukaryot Cell 8:1814–1827.
Tewari A, Fremont R, Khodakhah K (2017) It's not just the basal ganglia: cerebellum as a target for dystonia therapeutics. Mov Disord 32:1537–1545.
Torres GE, Sweeney AL, Beaulieu JM, Shashidharan P, Caron MG (2004) Effect of torsinA on membrane proteins reveals a loss of function and a dominant-negative phenotype of the dystonia-associated DeltaE-torsinA mutant. Proc Natl Acad Sci U S A 101:15650–15655.
Vander Heyden AB, Naismith TV, Snapp EL, Hanson PI (2011) Static retention of the lumenal monotopic membrane protein torsinA in the endoplasmic reticulum. EMBO J 30:3217–3231.
VanGompel MJ, Nguyen KC, Hall DH, Dauer WT, Rose LS (2015) A novel function for the *Caenorhabditis elegans* torsin OOC-5 in nucleoporin localization and nuclear import. Mol Biol Cell 26:1752–1763.
Vorlander MK, Pacheco-Fiallos B, Plaschka C (2022) Structural basis of mRNA maturation: time to put it together. Curr Opin Struct Biol 75:102431.
Walter W, Sanchez-Cabo F, Ricote M (2015) GOplot: an R package for visually combining expression data with functional analysis. Bioinformatics 31:2912–2914.
White SR, Lauring B (2007) AAA+ ATPases: achieving diversity of function with conserved machinery. Traffic 8:1657–1667.
Wing CE, Fung HYJ, Chook YM (2022) Karyopherin-mediated nucleocytoplasmic transport. Nat Rev Mol Cell Biol 23:307–328.
Xu Y, Lopes C, Qian Y, Liu Y, Cheng L, Goulding M, Turner EE, Lima D, Ma Q (2008) Tlx1 and Tlx3 coordinate specification of dorsal horn pain-modulatory peptidergic neurons. J Neurosci 28:4037–4046.
Zhang K, et al. (2015) The C9orf72 repeat expansion disrupts nucleocytoplasmic transport. Nature 525:56–61.
Zhang J, Weinrich JAP, Russ JB, Comer JD, Bommareddy PK, DiCasoli RJ, Wright CVE, Li Y, van Roessel PJ, Kaltschmidt JA (2017) A role for dystonia-associated genes in spinal GABAergic interneuron circuitry. Cell Rep 21:666–678.
Zhang S, Williamson NA, Duvick L, Lee A, Orr HT, Korlin-Downs A, Yang P, Mok YF, Jans DA, Bogoyevitch MA (2020) The ataxin-1 interactome reveals direct connection with multiple disrupted nuclear transport pathways. Nat Commun 11:3343.
Zhao C, Brown RS, Chase AR, Eisele MR, Schlieker C (2013) Regulation of Torsin ATPases by LAP1 and LULL1. Proc Natl Acad Sci U S A 110:E1545–1554.
Zufferey R, Dull T, Mandel RJ, Bukovsky A, Quiroz D, Naldini L, Trono D (1998) Self-inactivating lentivirus vector for safe and efficient in vivo gene delivery. J Virol 72:9873–9880.